Covalent hybrids based on Re(i) tricarbonyl complexes and polypyridine-functionalized polyoxometalate: synthesis, characterization and electronic properties

Thomas Auvray, Marie-pierre Santoni, Bernold Hasenknopf, Garry S Hanan

Covalent hybrids based on Re(I) tricarbonyl complexes and polypyridine-functionalized polyoxometalate: synthesis, characterization and electronic properties

Thomas Auvray,[a] Marie-Pierre Santoni,[b*] Bernold Hasenknopf,[c]* Garry S. Hanan[a]*

A series of $[Re(CO)_3Br(N^N)]$ (N^N = substituted 2,2'-bipyridine ligand) complexes based on polypyridine-functionalized Dawson polyoxometalate (**1-3**) has been synthesized. The new hybrids (**4-6**) were characterized by various analytical techniques, including absorption, vibrational and luminescence spectroscopies as well as electrochemistry. Both units, the polyoxometalate and the transition metal complex, retain their intrinsic properties. Their combination in the newly prepared hybrids results in improved photosensitization in the high-energy visible region. However, a complete quenching of the emission for the $[Re(CO)_3Br(N^N)]$ complexes is observed due to formation of a charge separated state, Re(II) – POM^-, as shown by quenching experiments as well as theoretical modelization via DFT.

Introduction

Polyoxometalates (POMs) are a class of anionic oxo-clusters of early-transition metals (mainly V(V), Mo(VI) and W(VI)) that exhibit a remarkable variety of structures and potential applications.[1] They have been used in catalysis, magnetism, material science and even medicine.[2] One of the most active areas of POM research focuses on their covalent functionalization to combine their unique properties with the properties of the grafted organic or organometallic components and develop new synergistic functionality in the hybrids.[3] This interest also arises from the analogy between POMs and metal oxide surfaces: POMs are considered as soluble analogues of metal oxides and, consequently, potential models for understanding elementary steps of heterogenous processes.[4] Among the covalent functionalization strategies, substitution of oxo ligand by poly-alcohol (triol and diol-amide, Figure 1b, 1c and 1e) is one of the most extensively used.[5] It has been applied to various POM structures (Lindqvist, Anderson and Dawson)[6] and the grafting reaction has been extensively studied.[7] While the use of diol-amide has been shown to induce electronic communication between the sub-unit of the prepared hybrids,[5c, 8] the use of triol such as tris-(hydroxymethyl) aminomethane (TRIS) has proven to be a viable route for the grafting of various moieties with limited electronic communication between the constitutive units,[9] in a true supramolecular approach.[10] We and others have used TRIS functionalized POMs to prepare polymeric[11] and discrete coordination species by introducing polypyridine ligands via an amide[12] or an imine[13] group. Many studies on covalently functionalized POMS aimed to combine them with known chromophores.[14] Both organics and organometallic dyes were explored, such as benzospiropyran[15], porphyrins,[9, 11b, 16] and Ru(II),[6c, 17] Ir(III)[18] and Re(I)[19] polypyridines complexes (Fig. 1).

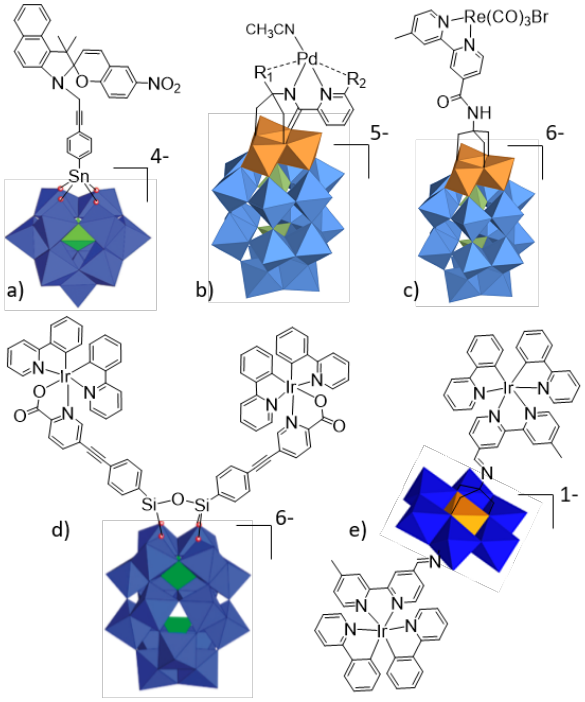

Figure 1. Chosen examples for different mode of grafting used to prepare covalently modified POMs (**a** Parrot et al.[15], **b** Riflade et al.[20], **c** Santoni et al.[19], **d** Matt et al.[18c] and **e** Streb et al.[18d])

Re(I) carbonyl diimine complexes have been the object of numerous studies in the past decades since the pioneering studies by Wrighton *et al.* of their photophysical properties.[21] Nowadays, these complexes are mostly being studied for their selective CO_2 to CO photocatalytic reduction abilities shown for the first time by Lehn *et al.*[22] They have also found application in other catalytic systems,[23] electroluminescent devices[24] and for biomedical purposes[25]. However, a few systems combining POM and Re(I) chromophore had been reported, based on non-covalent electrostatic interactions, such as counter-cation recognition via a crown-ether modified ligand,[26] or hydrogen bonding via a pendant amine on the Re complex.[27] We noted that there are several reports of Re carbonyl compounds based on POMs, in which the fac-$\{Re(CO)_3\}$ coordination sphere is completed by oxo or alkoxo

ligands from the POM skeleton.[28] While those compounds exhibit interesting structural and electronic properties due that unique coordination environment, they don't present metal-to-ligand charge-transfer (MLCT) bands as observed in the Re tricarbonyl diimine complexes such as *fac*-$[Re(CO)_3Br(bpy)]$ (where bpy is 2,2'-bipyridine).

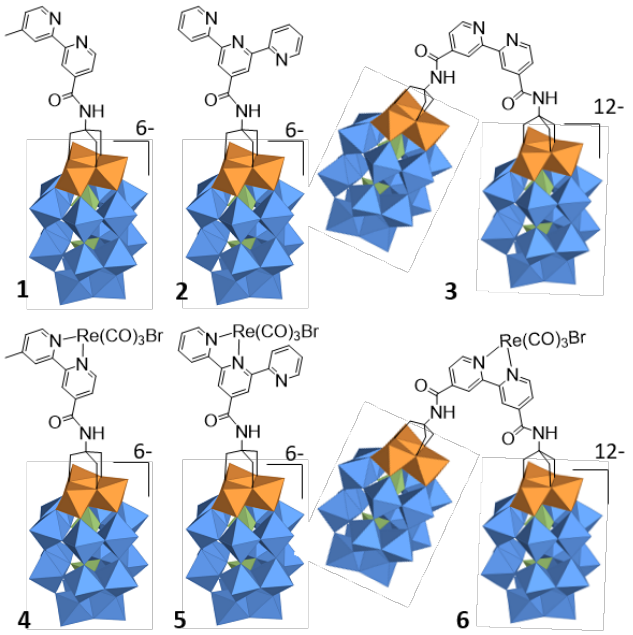

Figure 2. Structure of the discussed functionalized POMs (1-3) and their Re complexes (4-6) (Orange octahedron: $\{VO_6\}$, Blue octahedron: $\{WO_6\}$, Green tetrahedron: $\{PO_4\}$)

Herein, we extend the family of hybrids combining Re(I) carbonyl complexes and polypyridine-functionalized POMs, by complexation of the $\{Re(CO)_3Br\}$ moiety onto the available coordination site of covalently modified POMs. The bipyridine-functionalized Dawson (**1**), terpyridine-substituted (**2**) and bridging-bipyridine-substituted (**3**) act as ligand for Re(I) thus affording hybrids **4**-**6**.

Results and discussion

Synthesis and characterization of triol-functionalized polypyridine

To prepare the targeted hybrids, the triol moiety was introduced via trans-esterification on the ethyl-carboxylate functionalized polypyridine ligands with TRIS, followed by an intramolecular rearrangement.[29] The three ligands thus obtained had been previously reported either by us (**L1**, **L2**)[6c, 19] or by Cronin *et al.* (**L3**)[30]. The detailed synthetic pathways are described in the Supporting Information (SI). The identity of the compounds was confirmed by ESI-MS, ^{1}H and ^{31}P NMR spectra. The presence of amide groups was confirmed by singlets at 7.65, 7.81 and 7.69 ppm for **L1**, **L2** and **L3**, respectively. The amide also appears on the IR spectra through its characteristic C=O stretching vibration at 1644, 1658 and 1645 cm^{-1} (Fig. S2).

Synthesis and characterization of polypyridine-POM hybrids

Following published procedures,[6b, 6c] the triol functionalized ligands were grafted on the tri-substituted Dawson type POM $[P_2V_3W_{15}O_{62}]^{9-}$ **7**, affording compounds **1**, **2** and **3** (Fig. 2) with high yield by combining the ligands and starting POM in stoichiometric amounts and heating them in the dark for several days at 80°C in *N,N*-dimethylacetamide (DMAc). The starting POM **7** was obtained by condensation of sodium metavanadate with the tri-vacant Dawson phosphotungstate $[P_2W_{15}O_{56}]^{12-}$ whose reproducible preparation has been extensively studied by Finke *et al.*.[31] The TRIS-capped POM **8**, previously reported by Cronin *et al.*[32], was prepared in a similar way, as a reference. In all cases, the grafting takes place on the $\{V_3\}$ cap (Fig. 2-3), due to the higher basicity of the oxo ligands linked to V^V centers instead of W^{VI} center,[33] maintaining the C_3v geometry of the cluster as shown by the crystallographic structure (vide infra). The reaction requires several days to ensure that the three alkoxide groups have replaced bridging μ^2-oxo ligands.[7a] The identity of the three hybrids was confirmed by ESI-MS (see Fig. S6-S8, S12) and their purity by ^{1}H and ^{31}P NMR, as well as elemental analysis. When comparing their IR spectra with that of the starting POM **7**, two features allow to confirm the grafting of the organic unit : (i) the enlarged splitting between the M-O-M vibrations between 700 and 800 cm^{-1} [5a](Fig. S3), (ii) the additional vibration bands corresponding to the amide C=O, C-O stretching and the aromatic C=C stretching and bending modes (albeit with weak intensities when compared to the tetrabutylammonium (TBA) C-N stretching bands at 1482 cm^{-1}) (Fig. S3).

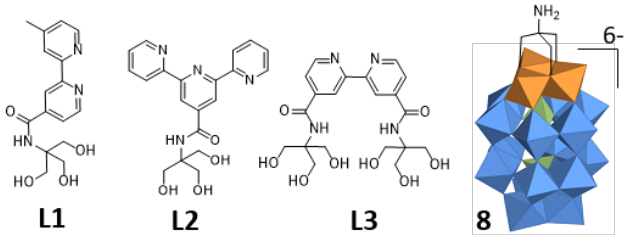

Figure 3. Structure of the polypyridine triol-functionalized ligands **L1-L3** and the reference TRIS-capped POM **8** (Orange octahedron: $\{VO_6\}$, Blue octahedron: $\{WO_6\}$, Green tetrahedron: $\{PO_4\}$)

When compared with the starting compound **7**, all the functionalized species exhibit a shift of both phosphate signals in their ^{31}P NMR spectra. This is mainly due to the decreased negative charge of the cluster after replacing the three oxo ligands by three alkoxo ligands. However, from one hybrid to another, there is almost no difference in the ^{31}P NMR spectra, indicating that there is almost no communication between the constitutive units, as expected for triol functionalized POM hybrids.

Complexation of {Re(CO)$_3$Br} on functionalized POMs

Compounds **4**, **5,** and **6** were obtained by combining one equivalent of Re(CO)$_5$Br with the corresponding functionalized POM in DMAc and heating the mixture overnight at 80°C in the dark. The complexation process was monitored by ^{1}H and ^{31}P NMR in CD$_3$CN as shown in Fig. 4. Upon complexation on **1** and **3**, the proton peaks of the bipyridine ligand are deshielded, as expected for this type of complex. In the case of compound **5**, the ^{1}H NMR spectrum becomes more complex when compared to hybrid **2** as the coordination on the terpyridine ligand only involves two of the pyridyls, thus making the external pyridyls inequivalent. This κ^2N coordination is expected as the formation of κ^3N terpyridine complexes typically requires high temperatures.[34] The coordination geometry is confirmed by

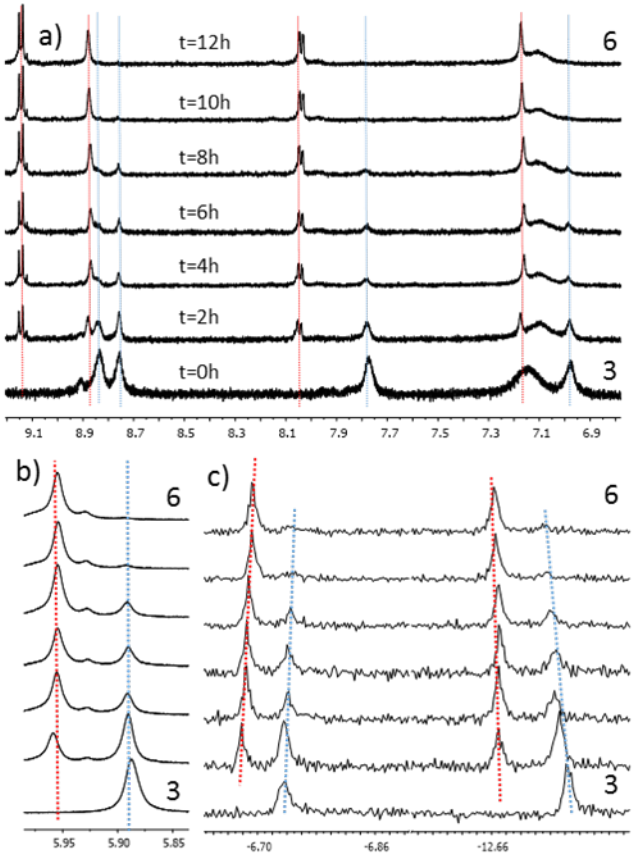

Figure 4. Follow-up of the complexation reaction using hybrid **3** in CD$_3$CN at 80°C. Spectra acquired every 2h. a) Aromatic region of the ^{1}H NMR, b) Methylene proton of the triol moiety and c) ^{31}P NMR

Table 1. CO stretching modes of compounds **4-6** as well as the reference **9**.

Compound	Wavenumber (σ / cm^{-1})
4	2019, 1916, 1891
5	2020, 1916, 1894
6	2023, 1925, 1899
9	2012, 1882, 1865

the presence of three distinct vibration bands arising from the carbonyl ligands as shown on the IR spectra of Fig S4. We also studied a known Re complex as a reference: we chose [Re(dmb)(CO)$_3$Br] (dmb = 4,4'-dimethyl-2,2'-bipyridine), referred as **9** hereafter. The values are tabulated in Table 1 and show that the carbonyl bands of **4-6** appear at higher frequency than in **9**. These shifts in wavenumber are in agreement with the stronger π-accepting character arising from the introduction of weakly electron-withdrawing amide group. The molecular formulas were confirmed by ESI-MS (Fig. S9-S11) and their purity checked by ^{1}H and ^{31}P NMR and EA.

Crystallographic study

We obtained crystals suitable for X-ray analysis by slow diffusion of di-isopropyl ether into an acetonitrile solution of **1**. It crystallizes in the orthorhombic space group $P2_12_12_1$ (complete details on the dataset and refinement are in the SI). The structure, presented in Fig. 5, confirms the expected grafting of the triol moiety by replacement of the three bridging μ^2-oxo ligands of the {V$_3$} cap by the μ^2-alkoxo groups. The non-crystallographic C$_3$v symmetry of the cluster is also unaffected, confirming the IR and NMR results.

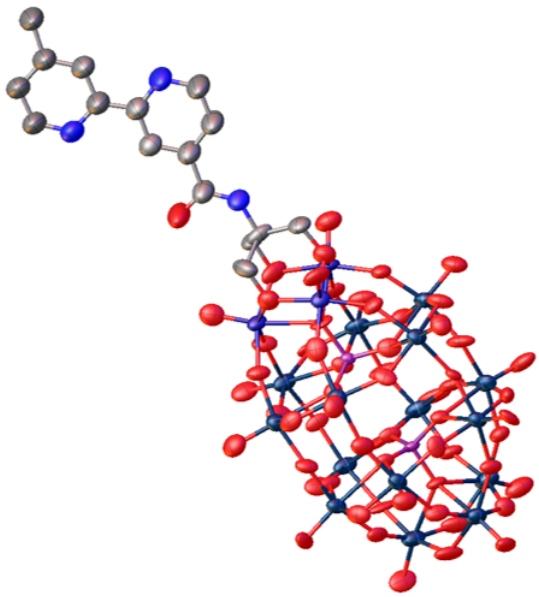

Figure 5. X-ray structure of compound **1** (Ellipsoids are at 50% probability. Hydrogens and counter cations are omitted for clarity)

UV-visible absorption and luminescence properties

The absorption spectra of the different compounds were collected: in both CH_3CN (Fig. 6) and DMF (Fig. S5b,c) for compounds **1-9** and only in DMF for the ligands (Fig. S5a), due to their insolubility in CH_3CN. Absorption maxima and molar absorption coefficient in CH_3CN are reported in Table 2.

The absorption spectra of the ligands are dominated by π→π* transitions in the UV part of the spectra. Noteworthy, **L3** absorbs at lower energy than the other ligands as expected from its stronger π-accepting character due to the presence of two amide groups. The native POM **7** exhibits intense absorption in the UV region, which is attributed to the multiple ligand-to-metal charge transfer ($O\rightarrow W^{VI}$ and $O\rightarrow V^{V}$ LMCTs), tailing into the high-energy part of the visible region (inset Fig. 5). Hybrid **8** exhibits similar absorption properties, as the TRIS fragment brings no additional transitions. The absorption spectra of the functionalized POMs **1-3** thus correspond to the combination of the LMCT transitions observed in **7** with the ligand centered (LC) transitions of the ligand, indicating minimal electronic communication between the two parts of the hybrid. Upon coordination of the $\{Re(CO)_3Br\}$ fragment, the LC transitions are slightly red-shifted while an additional transition emerges in the visible part of the spectra, corresponding to the Re(d)→π* metal-to-ligand charge transfer (MLCT). This additional transition leads to an increase of the molar absorption coefficient in the high energy visible region (*i.e* in the case of ε450, its value is almost twice as high in **6** as compared to **3**), as observed when comparing the insets of Fig. 5.

Re(I) bipyridine complexes are known to be emissive, displaying intense luminescence when excited in their ^{1}MLCT band. The reference compound **9**, for example, emits with a maximum at 584 nm,[35] while a complex based on a bis-amide bipyridine as in **6** has been reported to emit around 650nm.[36] However, in the case of our covalently modified POM based Re complexes, no luminescence could be detected upon excitation of the ^{1}MLCT transition (see Fig. S27). The causes of this complete luminescence quenching will be discussed below.

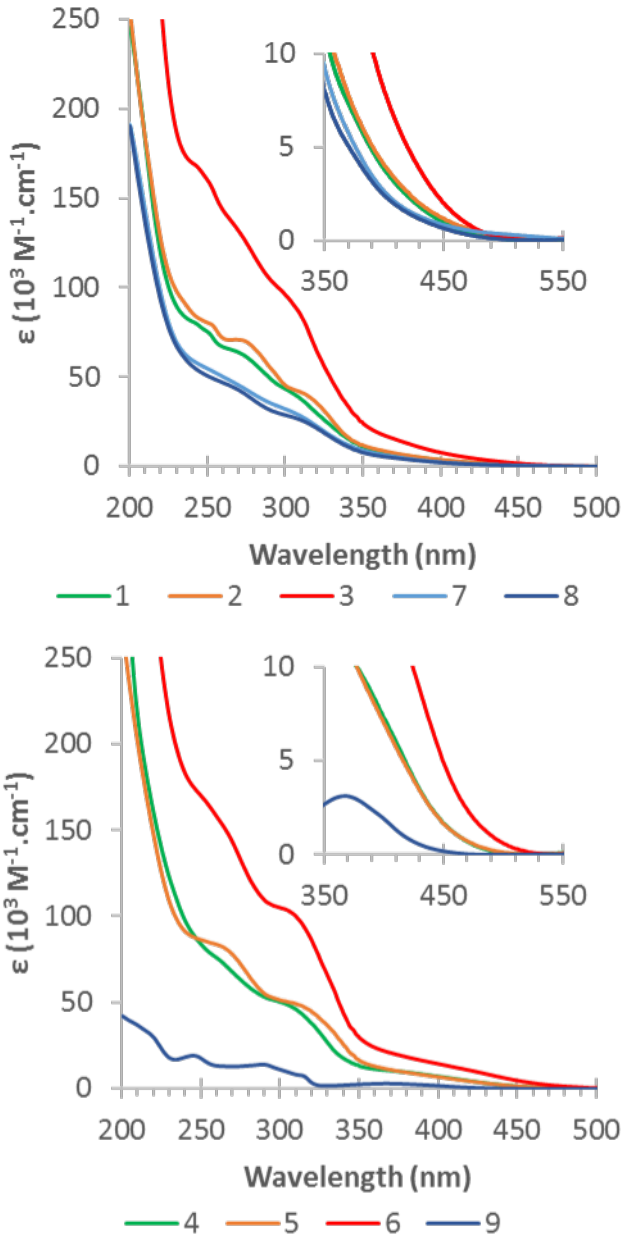

Figure 6. Absorption spectra at 298K in CH_3CN of compounds **1-9**.

Table 2. Absorption data for compounds **1-9**. All measurements were done in CH_3CN at RT.

Compounds	Absorption (λ/nm) (ε/10^3 M^{-1} cm^{-1})
1	308 (sh, 38.6), 269 (63.7), 251 (74.1), 241 (80.2)
2	314 (40.1), 272 (71.1), 253 (sh, 79.4)
3	307 (sh, 87.7), 269 (sh, 132.1), 247 (sh, 142,9)
4	375 (sh, 8.2), 304 (49.2), 260 (sh, 73.9)
5	381 (sh, 8.1), 313 (46.8), 264 (80.4)
6	381 (sh, 17.1), 305 (102.1), 263 (sh, 151.3)
7	309 (sh, 28.9), 258 (sh, 51.1)
8	315 (sh, 29.2), 270 (sh, 49.5)
9	372 (2.8), 314 (sh, 7.1), 290 (13.7), 218 (sh, 30.2)

Electrochemical studies

To confirm that the electronic communication between the complex and the cluster is negligible, the electrochemical properties of the different compounds were investigated using both cyclic voltammetry (CV) and square-wave (SW) measurements. The results are gathered in Table 3 while the cyclic voltammograms can be found in the SI (Fig S14-S25).
Regarding redox properties for the ligands, they all exhibit several reductions and one oxidation. **L1** is harder to reduce than **L3**, itself harder to reduce than **L2**, in agreement with the increasing electron-accepting character correlated to the additional amide group in the case of **L3** and the extended conjugation in the case of **L2**.

Table 3. Redox potentials of ligands **L1-L3**, hybrids **1-3** and **8**, POM **7** and Re complexes **4-6** and **9**.

Compound	Reductions (V vs SCE)	Oxidations (V vs SCE)
L1[a]	-1.78 (irr), -2.15 (qr,170), -2.46 (irr)	1.05 (irr)
L2[a]	-1.62 (qr, 280), -2.07 (qr, 200), -2.59 (irr)	0.92 (irr)
L3[a]	-1.72 (irr), -1.98 (qr, 80), -2.36 (irr)	0.88 (irr)
1[b]	0.25, -0.06, -0.75, -1.09, -1.51, -1.94, -2.23	-
2[b]	0.25, 0.01, -0.14, -0.78, -1.09, -1.50, -1.84, -2.23	-
3[b]	0.30, -0.51, -1.03, -1.28, -1.59, -1.77, -1.94	-
4[b]	0.38, -0.60, -1.08, -1.17, -1.56, -1.90, -2.24	0.88 (irr), 1.42 (irr), 1.88(irr)
5[b]	0.35, -0.61, -1.03, -1.13, -1.53, -1.80, -2.26	0.88 (irr), 1.33 (irr), 2.08(irr)
6[b]	0.36, -0.48, -0.97, -1.40, -2.32	0.90 (irr), 1.45(irr)
7[b]	0.37, 0.09, -0.81, -1.17, -1.45, -1.95, -2.24	-
8[b]	0.17, -0.04, -1.03, -1.48, -1.57, -1.95, -2.20	1.51 (irr)
9[c]	-1.41 (qr, 94), -1.80 (irr), -2.18 (irr), -2.50 (qr, 140)	0.86 (irr), 1.36(irr), 1.88 (irr)

All redox potentials were measured (V vs. SCE) at RT in degassed solutions with 1 mM of analyte and 0.1 M $TBAPF_6$ as supporting Electrolyte. [a] in DMF with Fc as internal reference (0.45V vs SCE), [b] in CH_3CN with AcFc as internal reference (0.71 V vs SCE), reduction potentials are extracted from SW experiments due to increased problems of adsorption of multi-charged species; [c] in CH_3CN with Fc as internal reference (0.40V vs SCE)

The oxidation process, also observed in **8**, is attributed to the triol moiety, as it was not observed in the model with a *tert*-butyl amide we reported elsewhere.[6c] The oxidation of compound **8** is harder than in the ligand due the electron withdrawing nature of the POM, thus confirming the existence of some communication, albeit with a limited spatial range as discussed by some of us on a similar system.[11b]

In the case of the POM based species, increasingly problematic adsorption phenomena on the glassy carbon electrode were observed upon reduction. Using CH_3CN instead of DMF reduced the impact of the adsorption, however, the redox processes remained ill-defined in some cases and the values in Table 3 are thus extracted from the SW measurements. In addition, ferrocene could not be used as an internal reference as it partially overlapped with the first reduction process and appeared to react with the reduced species produced. To increase the reference potential, we chose a derivative of ferrocene, namely acetyl-ferrocene (AcFc).[37]

The tri-vanadium substituted Dawson polyoxotungstate is a class I POM per Pope's classification.[38] According to previous electrochemical investigation,[5a, 11b, 33] the first three reduction processes take place on the three V^V centers. These reductions were described as two (mono and bi-electronic) or three separated waves. When compared to the starting POM **7**, the functionalized POMs **1**,**2**,**3** and **8** are reduced at lower potential. This shift of the first reduction shows that there is some electronic communication between the organic part and the POM. Indeed, one would expect the presence of an electron donating group such as the amine in **8** would make the reduction of the spatially close V^V center harder. Besides, the reduction is harder in the case of **8** than for **1-3**, in agreement with the reduced electron donating properties of the amine group once it is included in the amide function. However, the first V^V reduction is similar in the POM based Re complexes **4-6** and the native POM **7**. This can be explained by the further diminished electronic density on the amide function after coordination, as the $\{Re(CO)_3Br\}$ moiety is an electron withdrawing group, due to the back-electron transfer towards the carbonyls. Less attention has been given in the literature to the following reduction that are expected to take place on the W^{VI} centers. In their initial report, Pope *et al.* studied **7** in water and reported two polyelectronic reduction at -0.70V and -0.84V (vs Ag/AgCl), with 2 and 4 electrons involved, respectively.[33] In our hands, **7** gave a first W centered reduction at -0.81V (vs SCE in CH_3CN), with four additional reductions at lower potentials. Similar reductions are observed in our functionalized POMs and their equivalent Re complexes. Due to the adsorption problem encountered, we chose not to extend the discussion on these processes any further. Besides, we were unable to distinguish between ligand and POM based reductions as the ligand-based redox processes, monoelectronic, are hidden by the polyelectronic reductions on the cluster. To assign the oxidation potential observed for the Re complexes **4-6**, we referred to the study by Bullock *et al.* on the multiple oxidation processes of **9** in CH_3CN.[39] This work proved that a disproportionation reaction via a bromide-bridged intermediate dimer takes place after the oxidation to form the Re^{II} species around 1.3V. This disproportionation leads to the formation of an acetonitrile adduct, where the solvent is replacing the bromide anion. This acetonitrile complex is reversibly oxidized at higher potential (i.e. around 1.8V). Noteworthy, this adduct was not observed for

compound **6**. This is not surprising as the size of the compound should disfavour the dimerization step. The presence of free bromide is confirmed by the oxidation peak of the Br_2/Br^- couple around 0.88V. When compared to reference **9**, our POM based Re complexes **4-6** are slightly harder to oxidize, as expected due to the electron withdrawing nature of the ligand used.

Investigation of the luminescence quenching

Based on the reduction potentials described above, we propose that the absence of luminescence in compound **4**, **5** and **6** can be caused by intramolecular electron transfer, leading to a transient charge-separated excited state, relaxing to the ground state via back electron transfer. Indeed, using the Rehm-Weller equation, the excited state oxidation potential $E^*_{(ReII/Re^*I)}$ of the different compounds is estimated to be around 1.3 – (1240/650) = -0.6 V, thus lower in potential than the three vanadium centered reductions previously described.

To confirm this hypothesis, we decided to investigate the bimolecular luminescence quenching of **9** by **7** in solution, since the native POM **7** exhibits similar redox properties with the hybrid rhenium complexes **4-6**. Due to the overlapping absorption spectra leading to a strong inner-filter effect, we followed the quenching by measuring the lifetime variation of **9** (τ_0 = 73 ns). A diffusion limited quenching was observed with k_q = 5.9 x 10^9 $mol^{-1}.L.s^{-1}$. (Fig. S26) This result confirms the possibility of quenching by electron transfer which would be much more efficient and possibly faster in the prepared hybrids as the covalent link between Re complex and the functionalized POM favours the intramolecular electron transfer process, overcoming the diffusion rate limitation.

Theoretical calculations were also performed to model the electronic properties of **4** and obtain more insight into the different accessible excited states upon excitation of the Re(d)→π* ^{1}MLCT bands. Complex **9** was also investigated to verify the model validity and complete details on the computational data can be found in the SI.

The LUMOs are centered on the POM except LUMO+6 which is ligand centered, as shown in part in Fig. 6 and more extensively in Table S3, which displays the electronic contribution of the different units of **4** in the orbitals from LUMO+6 to HOMO-4.

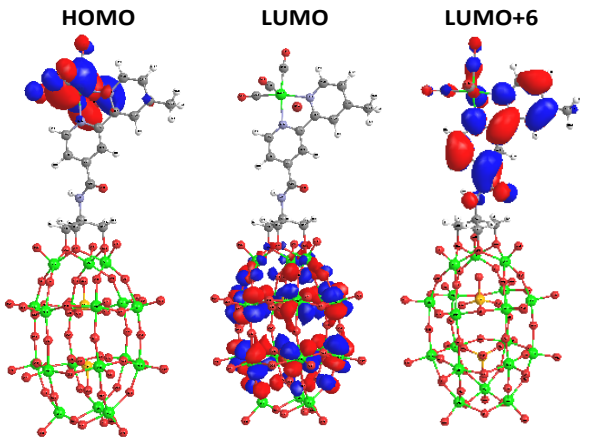

Figure 6. Selected Molecular Orbitals for **4** (Isovalue 0.03 e A^{-3})

Table 4. First predicted singlet and triplet transitions with their respective wavelength, main contribution, oscillator strength and attribution

S_0 to	λ(nm)	Contribution	Osc. Strength	Attribution
S_1/T_1	523	H→L	0	Re→POM CSS
S_2/T_2	511	H-1→L	0	Re→POM CSS
S_3/T_3	472	H→L+1	0	Re→POM CSS
S_4/T_4	471	H→L+2	0	Re→POM CSS
T_5	465	H→L+6	0	Re(d)→π* MLCT
S_5/T_6	463	H-1→L+1	0	Re→POM CSS
S_6/T_7	462	H-1→L+2	0	Re→POM CSS
T_{10}	453	H-1→L+6	0	Re(d)→π* MLCT
S_7	447	H-3→L	0	$O→V^V$(d) LMCT
S_8	446	H→L+6	0.004	Re(d)→π* MLCT
S_9	436	H-3→L+1	0.011	$O→V^V$(d) LMCT
S_{10}	423	H-1→L+6	0.091	Re(d)→π* MLCT

On the other hand, HOMO to HOMO-2 are centered on the {$Re(CO)_3Br$} moiety, while HOMO-3 and HOMO-4 have mixed contributions located around the triol-amide fragment, illustrating the limited range of electron delocalization as expected for a triol modified POM.[11b] Analysis of the TD-DFT results, presented in part in Table 4 (see Table S4 for complete data), confirm the attribution of the UV-vis transition proposed above and show the existence of several optically dark states surrounding the MLCTs and LMCTs transitions. The presence of these dark states, corresponding to effective charge separated states (CSS) (i.e. charge transfer from the {$Re(CO)_3Br$} moiety to the POM), is expected to facilitate electron transfer from the π* orbital of the bipyridine ligand to the vacant d orbitals on the POM after population of the $^{1/3}$MLCT levels. Noteworthy, the lowest CSSs appear to have mixed singlet and triplet nature, probably due to the strong spin-orbit coupling expected for third-row transition metal like Re and W. Similar results were obtained from the theoretical study conducted by Proust *et al.* on an Ir-POM hybrid.[18c] Based on these results, we propose the schematic energy diagram on Fig. 7 to explain the luminescence quenching by intramolecular charge transfer.

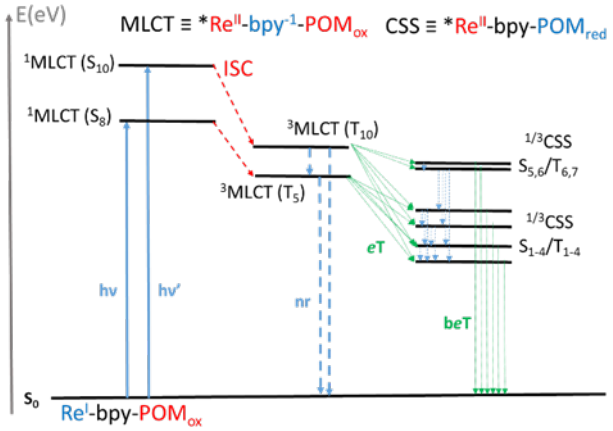

Figure 7. Energy diagram showing the pathway for luminescence quenching via intramolecular electron transfer. (nr : non-radiative, *e*T : electron transfer, b*e*T : back electron transfer, ISC : intersystem crossing)

Conclusion

Herein, we have reported the synthesis and characterization of three new hybrid Re^I carbonyl complexes based on polypyridine functionalized polyoxometalate. These covalent hybrids exhibit enhanced photosensitization in the visible, up to 500 nm, while maintaining the properties of each of their constitutive units. In all cases, the well documented emission arising from the ^{3}MLCT state of Re diimine complexes is quantitatively quenched. We proposed that an intramolecular electron transfer from the excited Re center to the POM is responsible for this quenching. We are currently investigating the possibility of using the theorized charge-separated state in photocatalytic reactions such as light-driven hydrogen production.

Acknowledgements

G.S.H. thanks the Natural Sciences and Engineering Research Council of Canada for financial support. T.A. thanks the Faculté des Études Supérieurs et Postdoctorales of Université de Montréal for an excellence scholarship. M.P.S. acknowledges financial support from Université Paris Diderot, Sorbonne Paris Cité and ITODYS. We are grateful to Compute Canada and WestGrid for access to computational resources and to the EA and XRD services at UdeM for their help. The authors wish to thank F. Schaper, A.L. Spek and D.J. Watkin for fruitful crystallographic discussions.

Notes and references

1. (a) M. T. Pope, *Heteropoly and Isopoly Oxometalates*, Springer-Verlag Berlin Heidelberg GmbH, 1983; (b) M. T. Pope and A. Müller, *Angew. Chem. Int. Ed.*, 1991, **30**, 34-48; (c) P. Gouzerh and M. Che, *L'actualité chimique*, 2006, **298**, 9-22.
2. (a) M. T. Pope and A. Muller, eds., *Topics in molecular organization and engineering*, Polyoxometalates : from platonic solids to anti-retroviral activity, Springer, 1994; (b) L. Cronin and A. Muller, eds., *Chem. Soc. Rev.*, Polyoxometalate cluster science (theme collection), 2012; (c) R. v. Eldik and L. Cronin, eds., *Advances in Inorganic Chemistry*, Polyoxometalate Chemistry, Elsevier, 2017; (d) C. L. Hill, ed., *Chem. Rev.*, Special Issue on polyoxometalates chemistry, 1998.
3. (a) A. Dolbecq, E. Dumas, C. R. Mayer and P. Mialane, *Chem. Rev.*, 2010, **110**, 6009-6048; (b) A. Proust, B. Matt, R. Villanneau, G. Guillemot, P. Gouzerh and G. Izzet, *Chem. Soc. Rev.*, 2012, **41**, 7605-7622; (c) M.-P. Santoni, G. S. Hanan and B. Hasenknopf, *Coord. Chem. Rev.*, 2014, **281**, 64-85; (d) A. Blazevic and A. Rompel, *Coord. Chem. Rev.*, 2016, **307**, 42-64; (e) G. Izzet, F. Volatron and A. Proust, *The Chemical Record*, 2017, **17**, 250-266.
4. (a) C. Streb, *Dalton Trans*, 2012, **41**, 1651-1659; (b) S. Piccinin, A. Sartorel, G. Aquilanti, A. Goldoni, M. Bonchio and S. Fabris, *Proc Natl Acad Sci U S A*, 2013, **110**, 4917-4922.
5. (a) Y. Hou and C. L. Hill, *J. Am. Chem. Soc.*, 1993, **115**, 11823-11830; (b) B. Hasenknopf, R. Delmont, P. Herson and P. Gouzerh, *Eur. J. Inorg. Chem.*, 2002, **2002**, 1081-1087; (c) J. Li, I. Huth, L. M. Chamoreau, B. Hasenknopf, E. Lacote, S. Thorimbert and M. Malacria, *Angew. Chem. Int. Ed.*, 2009, **48**, 2035-2038.
6. (a) A. Müller, J. Meyer, H. Bögge, A. Stammler and A. Botar, *Z. Anorg. Allg. Chem.*, 1995, **621**, 1818-1831; (b) Pierre R. Marcoux, B. Hasenknopf, J. Vaissermann and P. Gouzerh, *Eur. J. Inorg. Chem.*, 2003, **2003**, 2406-2412; (c) M. P. Santoni, A. K. Pal, G. S. Hanan, A. Proust and B. Hasenknopf, *Inorg. Chem.*, 2011, **50**, 6737-6745.
7. (a) H. Zeng, G. R. Newkome and C. L. Hill, *Angew. Chem. Int. Ed.*, 2000, **39**, 1771-1774; (b) E. F. Wilson, H. N. Miras, M. H. Rosnes and L. Cronin, *Angew. Chem. Int. Ed.*, 2011, **50**, 3720-3724; (c) P. Wu, P. Yin, J. Zhang, J. Hao, Z. Xiao and Y. Wei, *Chem. Eur. J.*, 2011, **17**, 12002-12005.
8. D. Lachkar, D. Vilona, E. Dumont, M. Lelli and E. Lacote, *Angew. Chem. Int. Ed.*, 2016, **55**, 5961-5965.
9. C. Allain, D. Schaming, N. Karakostas, M. Erard, J. P. Gisselbrecht, S. Sorgues, I. Lampre, L. Ruhlmann and B. Hasenknopf, *Dalton Trans*, 2013, **42**, 2745-2754.
10. J. M. Lehn, *Supramolecular Chemistry, Concepts and Perspectives*, VCH Verlagsgesellschaft mbH, 1995.
11. (a) S. Favette, B. Hasenknopf, J. Vaissermann, P. Gouzerh and C. Roux, *Chem. Comm.*, 2003, 2664-2665; (b) I. Azcarate, I. Ahmed, R. Farha, M. Goldmann, X. Wang, H. Xu, B. Hasenknopf, E. Lacote and L. Ruhlmann, *Dalton Trans*, 2013, **42**, 12688-12698; (c) A. Abhervé, M. Palacios-Corella, J. M. Clemente-Juan, R. Marx, P. Neugebauer, J. van Slageren, M. Clemente-León and E. Coronado, *J. Mater. Chem. C*, 2015, **3**, 7936-7945.
12. M. P. Santoni, A. K. Pal, G. S. Hanan, M. C. Tang, K. Venne, A. Furtos, P. Menard-Tremblay, C. Malveau and B. Hasenknopf, *Chem. Comm.*, 2012, **48**, 200-202.
13. C. Allain, S. Favette, L. M. Chamoreau, J. Vaissermann, L. Ruhlmann and B. Hasenknopf, *Eur. J. Inorg. Chem.*, 2008, **2008**, 3433-3441.
14. J. J. Walsh, A. M. Bond, R. J. Forster and T. E. Keyes, *Coord. Chem. Rev.*, 2016, **306**, 217-234.
15. A. Parrot, A. Bernard, A. Jacquart, S. A. Serapian, C. Bo, E. Derat, O. Oms, A. Dolbecq, A. Proust, R. Metivier, P. Mialane and G. Izzet, *Angew. Chem. Int. Ed.*, 2017, 10.1002/anie.201701860.
16. (a) A. Harriman, K. J. Elliott, M. A. H. Alamiry, L. L. Pleux, M. Séverac, Y. Pellegrin, E. Blart, C. Fosse, C. Cannizzo, C.

R. Mayer and F. Odobel, *J. Phys. Chem. C*, 2009, **113**, 5834-5842; (b) Z. Huo, D. Zang, S. Yang, R. Farha, M. Goldmann, B. Hasenknopf, H. Xu and L. Ruhlmann, *Electrochimica Acta*, 2015, **179**, 326-335.
17. B. Matt, C. Coudret, C. Viala, D. Jouvenot, F. Loiseau, G. Izzet and A. Proust, *Inorg. Chem.*, 2011, **50**, 7761-7768.
18. (a) B. Matt, J. Moussa, L.-M. Chamoreau, C. Afonso, A. Proust, H. Amouri and G. Izzet, *Organometallics*, 2012, **31**, 35-38; (b) B. Matt, J. Fize, J. Moussa, H. Amouri, A. Pereira, V. Artero, G. Izzet and A. Proust, *Energy Environ Sci*, 2013, **6**, 1504-1508; (c) B. Matt, X. Xiang, A. L. Kaledin, N. Han, J. Moussa, H. Amouri, S. Alves, C. L. Hill, T. Lian, D. G. Musaev, G. Izzet and A. Proust, *Chem. Sci.*, 2013, **4**, 1737; (d) S. Schönweiz, S. A. Rommel, J. Kübel, M. Micheel, B. Dietzek, S. Rau and C. Streb, *Chem. Eur. J.*, 2016, **22**, 12002-12005.
19. M. P. Santoni, A. K. Pal, G. S. Hanan, M. C. Tang, A. Furtos and B. Hasenknopf, *Dalton Trans.*, 2014, **43**, 6990-6993.
20. B. Riflade, J. Oble, L. Chenneberg, E. Derat, B. Hasenknopf, E. Lacôte and S. Thorimbert, *Tetrahedron*, 2013, **69**, 5772-5779.
21. M. Wrighton and D. L. Morse, *J. Am. Chem. Soc.*, 1974, **96**, 998-1003.
22. (a) J. Hawecker, J.-M. Lehn and R. Ziessel, *Chem. Comm.*, 1983, 536-538; (b) Y. Yamazaki, H. Takeda and O. Ishitani, *Journal of Photochemistry and Photobiology C: Photochemistry Reviews*, 2015, **25**, 106-137.
23. A. Zarkadoulas, E. Koutsouri, C. Kefalidi and C. A. Mitsopoulou, *Coord. Chem. Rev.*, 2015, **304-305**, 55-72.
24. T. Klemens, A. Świtlicka-Olszewska, B. Machura, M. Grucela, H. Janeczek, E. Schab-Balcerzak, A. Szlapa, S. Kula, S. Krompiec, K. Smolarek, D. Kowalska, S. Mackowski, K. Erfurt and P. Lodowski, *RSC Adv.*, 2016, **6**, 56335-56352.
25. R. Alberto, R. Schibli, R. Waibel, U. Abram and A. P. Schubiger, *Coord. Chem. Rev.*, 1999, **190-192**, 901-919.
26. J. Ettedgui, Y. Diskin-Posner, L. Weiner and R. Neumann, *J. Am. Chem. Soc.*, 2011, **133**, 188-190.
27. E. Haviv, L. J. Shimon and R. Neumann, *Chem. Eur. J.*, 2017, **23**, 92-95.
28. (a) P. Gouzerh, R. Villanneau, R. Delmont and A. Proust, *Chem. Eur. J.*, 2000, **6**, 1184-1192; (b) R. Villanneau, A. Proust, F. Robert and P. Gouzerh, *Chem. Eur. J.*, 2003, **9**, 1982-1990; (c) C. Zhao, W. Rodriguez-Cordoba, A. L. Kaledin, Y. Yang, Y. V. Geletii, T. Lian, D. G. Musaev and C. L. Hill, *Inorg. Chem.*, 2013, **52**, 13490-13495; (d) C. Zhao, E. N. Glass, J. M. Sumliner, J. Bacsa, D. T. Kim, W. Guo and C. L. Hill, *Dalton Trans*, 2014, **43**, 4040-4047; (e) J. Jia, Y. Zhang, P. Zhang, P. Ma, D. Zhang, J. Wang and J. Niu, *RSC Adv.*, 2016, **6**, 108335-108342; (f) J. Li, J. Guo, J. Jia, P. Ma, D. Zhang, J. Wang and J. Niu, *Dalton Trans*, 2016, **45**, 6726-6731.
29. G. R. Newkome, G. R. Baker, S. Arai, M. J. Saunders, P. S. Russo, K. J. Theriot, C. N. Moorefield, L. E. Rogers and J. E. Miller, *J. Am. Chem. Soc.*, 1990, **112**, 8458-8465.
30. C. P. Pradeep, F. Y. Li, C. Lydon, H. N. Miras, D. L. Long, L. Xu and L. Cronin, *Chem. Eur. J.*, 2011, **17**, 7472-7479.
31. (a) R. G. Finke, B. Rapko, R. J. Saxton and P. J. Domaille, *J. Am. Chem. Soc.*, 1986, **108**, 2947-2960; (b) W. W. Laxson, S. Ozkar and R. G. Finke, *Inorg. Chem.*, 2014, **53**, 2666-2676.
32. C. P. Pradeep, D. L. Long, G. N. Newton, Y. F. Song and L. Cronin, *Angew. Chem. Int. Ed.*, 2008, **47**, 4388-4391.
33. S. P. Harmalker, M. A. Leparulo and M. T. Pope, *J. Am. Chem. Soc.*, 1983, **105**, 4286-4292.
34. (a) E. W. Abel, V. S. Dimitrov, N. J. Long, K. G. Orrell, A. G. Osborne, H. M. Pain, V. Sik, M. B. Hursthouse and M. A. Mazid, *Chem. Comm.*, 1993, 597-603; (b) B. Laramée-Milette, N. Zaccheroni, F. Palomba and G. S. Hanan, *Chem. Eur. J.*, 2017, **23**, 6370-6379.
35. C. Bruckmeier, M. W. Lehenmeier, R. Reithmeier, B. Rieger, J. Herranz and C. Kavakli, *Dalton Trans*, 2012, **41**, 5026-5037.
36. C. Liu, K. D. Dubois, M. E. Louis, A. S. Vorushilov and G. Li, *ACS Catalysis*, 2013, **3**, 655-662.
37. J. R. Aranzaes, M.-C. Daniel and D. Astruc, *Can. J. Chem.*, 2006, **84**, 288-299.
38. M. T. Pope, *Inorg. Chem.*, 1972, **11**, 1973-1974.
39. J. P. Bullock, E. Carter, R. Johnson, A. T. Kennedy, S. E. Key, B. J. Kraft, D. Saxon and P. Underwood, *Inorg. Chem.*, 2008, **47**, 7880-7887.